XMM-NEWTON DETECTION OF VELOCITY STRUCTURE IN THE CORE OF ABELL 2597

Martin Still[a b], Richard Mushotzky[a]

[a]NASA/Goddard Space Flight Center, Greenbelt MD 20771, USA

[b]Universities Space Research Association

RGS observations of Abell 2597 show that the redshift of the cluster core is inconsistent with the mean redshift of cluster members. Spectral line profiles suggest a hybrid model of a hot, extended plasma plus a cool, point-like core, blueshifted relative to the cluster mean. Acceptable fits are obtained from this model assuming two simple thermal plasma distributions. From this model, the velocity of the core and the mean cluster redshift are inconsistent with > 99.9 percent confidence.

1. Observations

XMM-Newton observed Abell 2597 between 03:29 UT and 09:20 UT during 2000 Nov 30. RGS spectra were extracted using the standard channel binning. The cross-dispersion extraction region was defined to include 98 percent of the flux within the RGS psf. With a 5 arcmin field of view in the cross-dispersion direction, this allowed sky regions to be extracted, albeit with reduced signal-to-noise compared to point source data and with some contamination from the outer regions of the cluster.

2. Results

First order RGS spectra are plotted in Fig. 1, revealing detections of O VIII Lyα, L-shell Fe transitions and, marginally, Si XIV Lyα.

2.1. Line velocities

Because the source is extended, there is a range of incident angles on the gratings and lines are consequently broadened. In order to fit the line profiles adequately we simulate the instrumental broadening by convolving spectral models with the spatial profile of the source in the dispersion direction of the RGS cameras. This is achieved with the package *rgsxsrc*, added to the XSPEC package for version 11.2. The algorithm generates a convolution function by integrating an image of the source over the cross-dispersion direction. In this case we have used a 0.35-2.5 keV image, extracted from the MOS1 events list. Although fast computationally, the disadvantage of this model is that the emitted spectrum is assumed to have uniform temperature across the source.

To measure the redshift of the Lyα O VIII line we use a Gaussian model, with a powerlaw to represent the continuum across the wavelength range 19–22Å. The best fit model, convolved with the spatial profile above, is plotted in Fig. 2. We take the rest-energy of the line as 653.6 eV (Johnson & Soff 1985) and assume the intrinsic width of the line is negligible. The redshift of this feature is consequently $z = 0.081^{+0.002}_{-0.004}$ ($\chi^2 = 51$ for 52 d.o.f.), where the errors are 90 percent confidence limits. This is less than the mean optical redshift of the cluster $z = 0.0852$ (Struble and Rood 1999) with greater than 99 percent confidence.

An identical model, ray-traced through a simulation of the *XMM-Newton* telescope using the Monte Carlo code discussed in Peterson *et al.* (2001), yields a consistent fit of $z = 0.078 \pm 0.001$. While the result is not particularly sensitive to the spatial distribution of the source, here we fit the data in the spatial direction as a β-function, where the spatial profile has an index of 0.62 and core radius of 27 arcmin.

A convolved Gaussian model fit to the suspected Lyα Si XIV line over the $\lambda\lambda$5–8Å range provides $z = 0.078^{+0.006}_{-0.009}$ ($\chi^2 = 52$ for 52 d.o.f.), taking the rest wavelength as 2.005 keV. This is consistent with the O VIII redshift and inconsistent with the optical redshift with 90 percent confidence.

To fit the Fe L shell transitions we adopt a neutrally-absorbed thermal plasma model (*vapec*; Brickhouse *et al.* 2000) over $\lambda\lambda$8–15Å, convolved with the MOS1 spatial profile. Photo-electric cross-sections were provided by

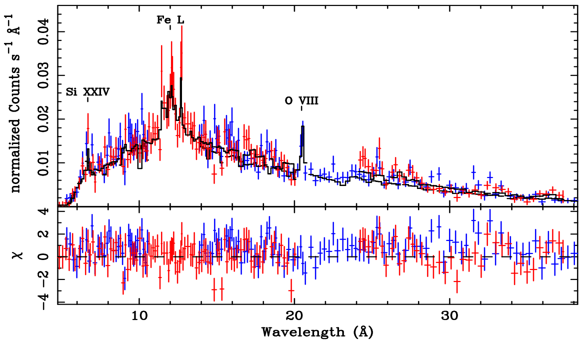

Figure 1. RGS1 (blue) and RGS2 (red) spectra of Abell 2597. The black lines correspond to a multiple thermal plasma fit, described in Sec. 2. Lines from O VIII, Fe XXIII, Fe XXIV, and possibly Si XIV are detected.
.

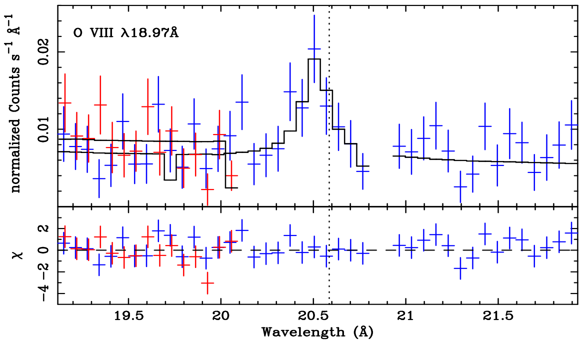

Figure 2. RGS1 (blue) and RGS2 (red) spectra of the O VIII line from Abell 2597. The black lines correspond to a powerlaw + Gaussian fit, convolved with the 0.35–2.5 keV MOS1 spatial profile. The redshift of the line corresponds to $z = 0.08$.

Balucinska-Church & McCammon (1992). Best fit parameters are $z = 0.086^{+0.004}_{-0.005}$, $n_H = 4^{+6}_{-4}\times10^{20}$ cm^{-2} and $kT = 3.1^{+1.0}_{-0.8}$ keV, with an Fe abundance of $0.44^{+0.32}_{-0.19}$ solar ($\chi^2 = 189$ for 179 d.o.f.). The redshift of the Fe lines are consistent with the mean optical redshift of the cluster. However there is one strong line at λ12.7Å that is not fit well by the model. This is because it is both blue-shifted relative to the model and narrower than the MOS1 convolution function. An additional Gaussian model component with negligible intrinsic width, broadened only by the point source response function, was applied to fit this feature. It is likely this line is either Fe XXII λ11.770Å at $z = 0.080^{+0.004}_{-0.004}$ or Fe XXIII λ11.736Å at $z = 0.082^{+0.004}_{-0.004}$ (Brown *et al.* 2002).

The RGS2 chip gap between λλ13.1–13.2Å may overlap another strong line. The current model is fitting solar abundance Ne X Lyα to the red wing of the feature, but this line equally may be Fe XXI λ12.284Å, which would reduce the temperature of the model considerably. by removing Ne from the model completely, best fit thermal plasma parameters are $z = 0.085^{+0.003}_{-0.006}$, $n_H = 9^{+12}_{-4}\times10^{20}$ cm^{-2} and $kT = 2.0^{+0.6}_{-0.6}$ keV, with an Fe abundance of $0.22^{+0.14}_{-0.10}$ solar ($\chi^2 = 187$ for 179 d.o.f.). The temperature is still too high to produce significant amounts of Fe XXI (Arnaud & Rothenflug 1985), but in reality, the source has a range of plasma temperatures (Sec. 2.2), while the fit converges on a mid-range value. Furthermore the narrow Fe XXII/Fe XXIII line is not being fit correctly by the instrumentally-broadened model, increasing the model temperature.

In collisional conditions, the absence of ionization states of Fe XX and below indicates plasma temperatures > 1 keV, while if Fe XXII is the cut-off state, the plasma temperature must be > 1.5 keV (Arnaud & Rothenflug 1985).

In summary, the hot Fe XXIV lines have velocities consistent with the mean optical redshift of the cluster. The unblended O VIII and Si XIV Lyα lines are blueshifted relative to the mean redshift with > 90 percent confidence. The cooler Fe transition, either Fe XXII or Fe XXIII is a narrow spectral feature. Its energy is consistent with both the optical mean and O VIII line velocities within the 90 percent confidence limit, but favours the O VIII redshift statistically.

2.2. A two-zone model

Fe transitions of different widths suggest that these lines are distributed differently in the source. This is reasonable considering Abell 2597 has a suspected cooling flow and the Fe line widths are as expected phenomenologically, where the broad lines arise in the hot, outer flow while the narrow lines originate in the cooler, inner flow. Inspection of the corresponding EPIC

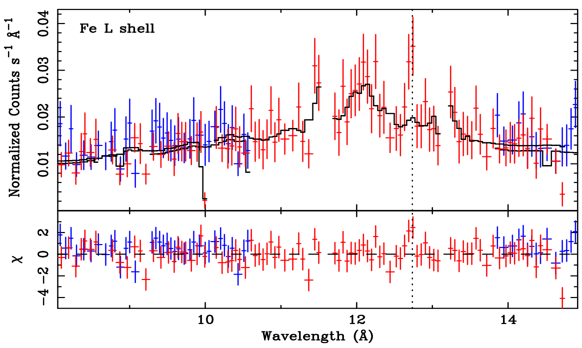

Figure 3. RGS1 (blue) and RGS2 (red) spectra of the Fe L complex from Abell 2597. The black lines correspond to an absorbed thermal plasma model (*vapec*) fit, convolved with the 0.35–2.5 keV MOS1 spatial profile.

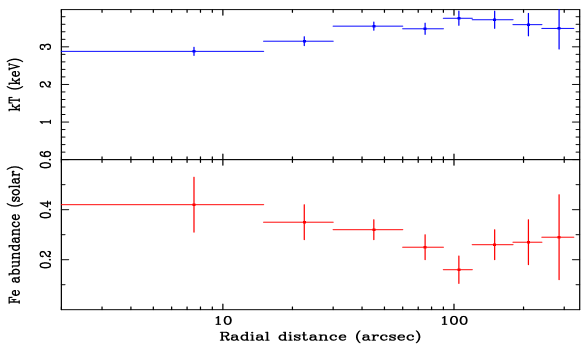

Figure 4. Temperature and abundance structure of Abell 2597, taken from *vapec* fits to the EPIC data.

data indeed shows a trend of decreasing temperature towards the center of the cluster (Fig. 4). If this model is correct, the core of the cluster has a peculiar velocity, relative to the cluster mean.

Whereas the Fe XXII and Fe XXIII ionization states have relatively narrow distributions over temperature, H-like O and Si have distributions considerably broader, with ranges encompassing Fe XXI–XXIV. Consequently, the O and Si lines could arise in both the inner and outer regions of the source. This is in fact a requirement for the O VIII Lyα transition in the context of this model, the outer region is responsible for the broad wings of the line, while a narrow core from the inner region produces the observed peculiar velocity.

A first order approximation to this is a two-zone model. The outer zone is an extended thermal plasma which we model using the MOS1 convolution function. The inner zone is a thermal plasma modeled as a point source. Both zones are absorbed by the same galactic neutral hydrogen column in the direction of the source, n_H = 2.49×10^{20} cm^{-2} (Dickey & Lockman 1990). Plasma parameters for the outer zone were fixed at values determined from EPIC spectral fitting (Fig. 4). Using the EPIC events, the source was found to be approximately isothermal, with no abundance gradients, at radii $>$ 1 arcmin from the center. We take $kT_\circ$ = 3.5 keV and element abundances [Fe/H] = -0.42 and [O/H] = -0.32. The redshift of the outer zone is fixed at the mean optical redshift of the cluster, $z_\circ = 0.0852$. Free floating parameters for this component are the normalization and the Si abundance which, being poorly constrained by the EPIC data, is tied to the Si abundance of the point source component to reduce redundancies. The temperature, kT_i, Fe, O and Si abundances, normalization and redshift, z_i are free floating parameters for the inner zone component. In order to fit the Fe XXII/Fe XXIII feature at λ11.7Å, Ne abundance must be significantly lower than solar. But it cannot be well constrained due to the RGS2 chip gap between $\lambda\lambda$13.1–13.2Å, so we assume it is negligible.

Table 1
Best fit parameters for the inner, point-like component of the two-zone emission model for Abell 2597.

kT_i	$1.6^{+0.2}_{-0.1}$ keV
[Fe/H]	$-0.32^{+0.16}_{-0.17}$
[O/H]	$-0.46^{+0.29}_{-0.76}$
[Si/H]	$+0.08^{+0.15}_{-0.23}$
z_i	$0.080^{+0.001}_{-0.001}$

Best fit parameters are provided in Table 1 and the best fit model spectrum is plotted over the data in Fig 1. z_i is less than the mean optical redshift with $>$ 99.9 percent confidence.

3. RGS wavelength scale

In this section we discuss whether the observed peculiar velocity could result from a pointing error. There is a small discrepancy between the location of the cD galaxy in the Digitized Sky Survey (spatially consistent with the brightest knot in the high resolution *Chandra* ACIS image; Fabian *et al.* 2001) and the position of the source in the OM images. This is most likely a symptom of the telescope pointing accuracy, which is limited to ~ 5 arcsec. With a position angle of 247 degrees, the disparity is ~ 0.4 arcsec in the dispersion direction of the RGS detector. To determine what effect an off-axis pointing on these scales will have on the point-source wavelength scale, we consider the derivative of the dispersion equation

$$\Delta\lambda = d \sin\alpha_0 \Delta\alpha \tag{1}$$

using a nominal incidence angle of $\alpha_0 = 1.5762$ degrees and a grating groove density of $d^{-1} = 645.6$ lines mm^{-1}. After correction for optical geometry the angular discrepancy is $\Delta\alpha = 0.45$ arcsec. This yields a drift in the wavelength scale at O VIII Lyα of $\Delta\lambda = 1$ mÅ. The observed velocity shift at the O VIII line corresponds to $\Delta\lambda \simeq 100$ mÅ. To obtain this through wavelength scale drift alone, we require a pointing offset by 48 arcsec. Erroneous pointing cannot account for the velocity shift observed.

4. Cluster velocity distribution

It would be constructive to compare $\Delta\lambda$ above with the measured velocity dispersion of Abell 2597 cluster members. The redshift of Abell 2597, $z = 0.0852$, is taken from the catalogue of Struble and Rood (1999) and it originates from the optical radial velocities of three cluster members, none of which are the cD galaxy, obtained by Kowalski, Ulmer and Cruddace (1983). These quantities have been corrected to the Local Group local standard of rest. To similarly correct our own results we must add 140 km s^{-1} (Courteau and van den Bergh 1999). This removes just 10 percent of the discrepancy between the X-ray line and optical measurements. The standard deviation between the three galactic velocities, $z = 2\times10^{-3}$, is of the same order as $\Delta\lambda$, but also of the same order as the systematic uncertainty introduced by using different cross-correlation templates in the optical redshift measurements. Therefore this comparison will be improved greatly after the Sloan Survey visits the cluster (Stoughton *et al.* 2002).

There has been an independent measure of the radial motion of the cD galaxy itself of $z = 0.0822$, accurate to the third significant digit (Owen, Ledlow and Keel 1995). Although still not consistent with the RGS measurement, it is significantly smaller than the mean cluster velocity.

5. Conclusion

The redshift of the core of Abell 2597 as measured by the RGS, is inconsistent with the mean redshift of member galaxies, suggesting that the cluster is not in a relaxed state.

REFERENCES

1. Arnaud M., Rothenflug R., 1985, A&AS, 60, 425
2. Balucinska-Church M., McCammon D., 1992, ApJ, 400, 699
3. Brickhouse N.S., Dupree A.K., Edgar R.J., Liedahl D.A., Drake S.A., White N.E., Singh K.P., 2000, ApJ, 530, 387
4. Brown G.V., Beiersdorfer P., Liedahl D.A., Widmann K., Kahn S.M., Clothiaux E.J., 2002, ApJS, 140, 589
5. Courteau S., van den Bergh S., 1999, AJ, 118, 337
6. Dickey J.M., Lockman F.J., 1990, ARAA. 28, 215
7. Fabian A.C. et al., 2001, MNRAS, 321, L33
8. Johnson W.R., Soff G., 1985, Atom. Data Nucl. Data Tables, 33, 405
9. Kowalski M.P., Ulmer M.P., Cruddace R.G., 1983, ApJ, 268, 540
10. Owen, F.N., Ledlow M.J., Keel W.C., 1995, AJ, 109, 14
11. Peterson J.R. et al., 2001, A&A, 365, L104
12. Stoughton C. et al., 2002, AJ, 123, 485
13. Struble M.F., Rood H.J., 1999, ApJS, 125, 35

ACKNOWLEDGEMENTS

Based on observations obtained with *XMM-Newton*, an ESA science mission with instruments and contributions directly funded by ESA Member States and the USA (NASA). Local Group velocity data were obtained from the NASA/IPAC Extragalactic Database. The *rgsxsrc* model was authored by A. Rasmussen.